Electronic Structure, Chemical Bonding, and Jahn−Teller Distortions in $CdPS_3$

Vladlen Zhukov,*,†,‡ Florent Boucher,§ Pere Alemany,|| Michel Evain,*,§ and Santiago Alvarez*,†

Departament de Química Inorgànica and Departament de Química Física, Universitat de Barcelona, Diagonal 647, 08028 Barcelona, Spain, and Institut des Matériaux de Nantes, CNRS UMR 0110, 2 rue de la Houssinière, 44072 Nantes Cedex 03, France

Received July 21, 1994[⊗]

The electronic band structure of and the chemical bonding in $CdPS_3$ have been studied by means of the self-consistent *ab initio* LMTO-ASA and the semiempirical tight-binding extended Hückel methods. The reluctance of the Cd atoms to occupy the center of the octahedral S_6 sites and their tendency to be displaced along the crystallographic *c* direction result from a second-order Jahn−Teller effect involving the Cd 5p and possibly the 5s orbitals. The high-temperature monoclinic modification of the $CdPS_3$ structure presents donor−acceptor interactions between the HOMO's and LUMO's of the $P_2S_6^{4-}$ species in neighboring layers, which are absent in the low-temperature rhombohedral phase. The off-center shift of the Cd atoms in the low-temperature phase has no relationship to the change in stacking pattern associated with the phase transition.

Introduction

The ternary thiophosphates and selenophosphates MPX_3, first synthesized by Friedel,[1] have been extensively studied after Klingen *et al.* established by X-ray diffraction the lattice parameters for a number of such compounds.[2] Further crystallographic studies have kept the size of this family continuously growing with more structures of thiophosphates[3−7] and selenophosphates[8−12] of transition and post-transition metals. These compounds present layered structures in which the two-dimensional slabs can be described as close-packed arrangements of sulfide ions with P_2^{8+} and M^{2+} ions occupying the octahedral holes. In the case of $CdPS_3$, an ABCABC stacking is found in the high-temperature monoclinic phase[6] (Figure 1, above). An ABAB stacking of the sulfides results in a rhombohedral structure found at low temperature[6] (schematically represented as a projection along the *b* direction in Figure 1, below). The phase transition between the two structures of $CdPS_3$ occurs at −45 °C.

Particular interest has been devoted to the anomalously high thermal displacement parameters found for the metal atom in a variety of MPS_3 and $MM'P_2S_6$ compounds.[6,7,13−15] In particular,

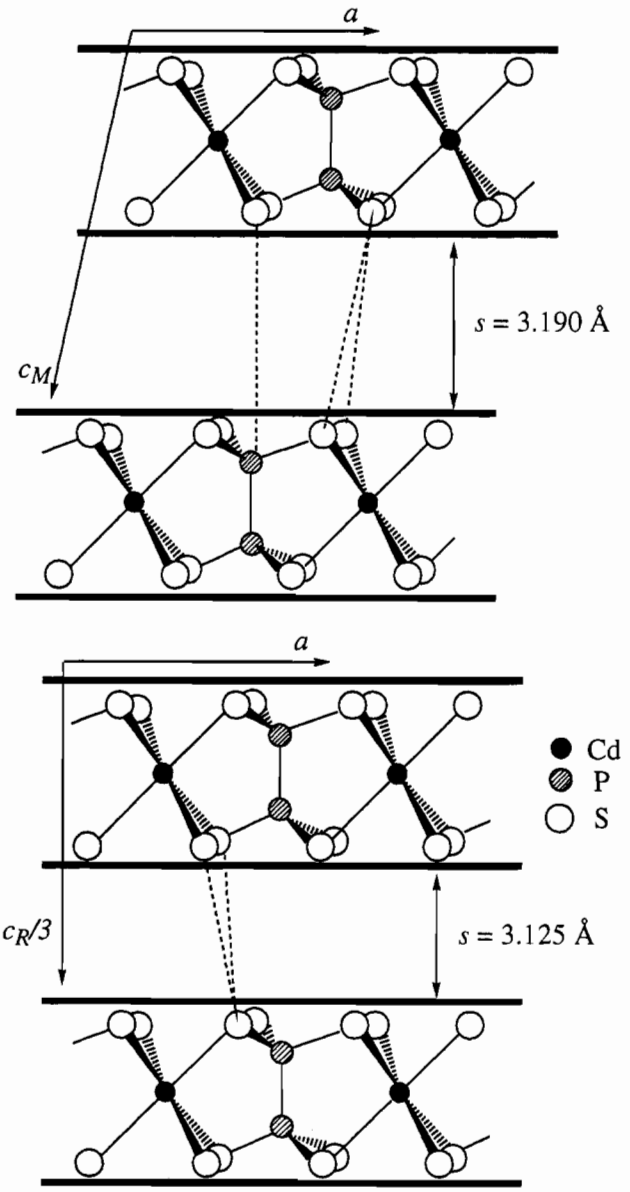

Figure 1. Schematic representations of the stacking patterns found in the monoclinic (high temperature, above) and rhombohedral (low temperature, below) phases of $CdPS_3$ viewed along the *b* axis.

† Departament de Química Inorganica, Universitat de Barcelona.
‡ On leave from the Institute of Solid State Chemistry, Urals Branch of the Academy of Sciences, Pervomayskaya 91, 620219 Ekaterinburg, Russia.
§ Institut des Matériaux de Nantes.
|| Departament de Química Física, Universitat de Barcelona.
⊗ Abstract published in *Advance ACS Abstracts,* January 15, 1995.

(1) Friedel. *C. R. Hebd. Seances Acad. Sci.* **1894**, *119*, 260.
(2) Klingen, W.; Eulenberger, G.; Hahn, H. *Naturwissenschaften* **1968**, *55*, 229.
(3) Klingen, W.; Eulenberger, G.; Hahn, H. *Z. Anorg. Allg. Chem.* **1973**, *401*, 97.
(4) Ouvrard, G.; Brec, R.; Rouxel, J. *Mater. Res. Bull.* **1985**, *20*, 1181.
(5) Prouzet, E.; Ouvrard, G.; Brec, R. *Mater. Res. Bull.* **1986**, *21*, 195.
(6) Boucher, F. These de doctorat, Université de Nantes, 1993.
(7) Boucher, F.; Evain, M.; Brec, R. *J. Alloys Compd.* **1994**, *215*, 63.
(8) Klingen, W.; Ott, R.; Hahn, H. *Z. Anorg. Allg. Chem.* **1973**, *396*, 271.
(9) Carpentier, C. D.; Nitsche, R. *Mater. Res. Bull.* **1974**, *9*, 401.
(10) Jandali, M. Z.; Eulenberger, G.; Hahn, H. *Z. Anorg. Allg. Chem.* **1978**, *447*, 105.
(11) Wiedenmann, A.; Rossat-Mignot, J.; Louisy, A.; Brec, R.; Rouxel, J. *Solid State Commun.* **1981**, *40*, 1067.
(12) Brec, R.; Louisy, A.; Ouvrard, G.; Verbaere, A.; Rouxel, J. *Rev. Chim. Miner.* **1982**, *19*, 497.
(13) Barj, M.; Lucazeau, G.; Ouvard, G.; Brec, R. *Eur. J. Solid State Inorg. Chem.* **1988**, *25*, 449.
(14) Brec, R.; Ouvrard, G.; Rouxel, J. *Mater. Res. Bull.* **1985**, *20*, 1257.
(15) Brec, R. *Solid State Ionics* **1986**, *22*, 3.

0020-1669/95/1334-1159$09.00/0

the probability density function (pdf) in the high-temperature phase of $CdPS_3$ is elongated along the c direction, and the structure refinement clearly revealed two Cd modes displaced 0.1 Å from the Cd mean positions, i.e., the center of the S_6 octahedra. In the low-temperature phase, the Cd atoms appear ordered and occupy alternative positions above and below the center of the octahedra. Also, in the analogous compound $AgScP_2S_6$, the Ag atom shows an abnormally large thermal parameter.[16] In both cases, the apparent off-center displacement of the metal atom was attributed to a second-order Jahn–Teller effect involving the filled d orbitals,[7,16] but no calculations were reported to support such assertion.

Among the theoretical studies performed on this family of compounds, Kurita and Nakao[17] reported band structure calculations for M = Mn, Fe, Ni. These authors studied different magnetic structures, optical properties, and the mechanism for Li intercalation. Whangbo[18] and Canadell[19] have reported extended Hückel tight-binding (EHTB) band calculations for MPS_3 systems, focusing mostly on transition metal compounds. A detailed orbital analysis of the structural off-center preference of several metal ions, however, has not been previously studied. In consequence, we have undertaken a theoretical study of the electronic structure of $CdPS_3$ and of the second-order Jahn–Teller effect related to the off-center displacement of the Cd ions. To this end, band calculations were performed at two different levels of approximation: the *ab initio* linear muffin-tin orbital method (LMTO) and the semiempirical one-electron extended Hückel method (see Computational Aspects for details).

Electronic Structure

For a simplified, symmetry-based analysis of the second-order Jahn–Teller (SOJT) effect, we consider an idealized octahedral

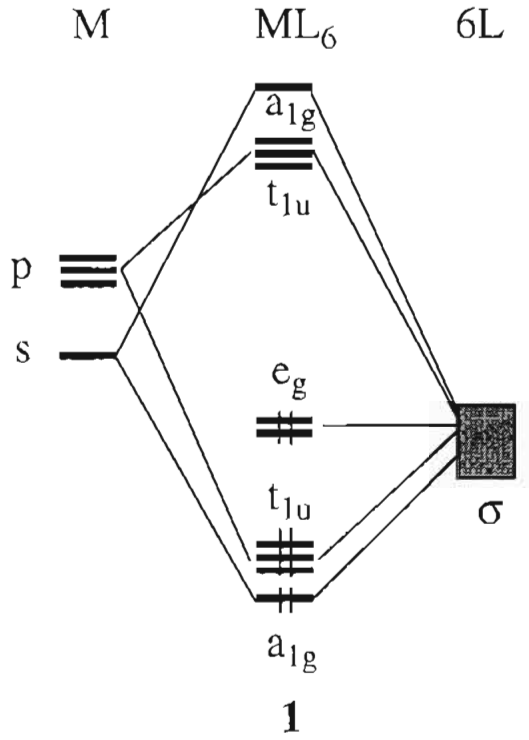

1

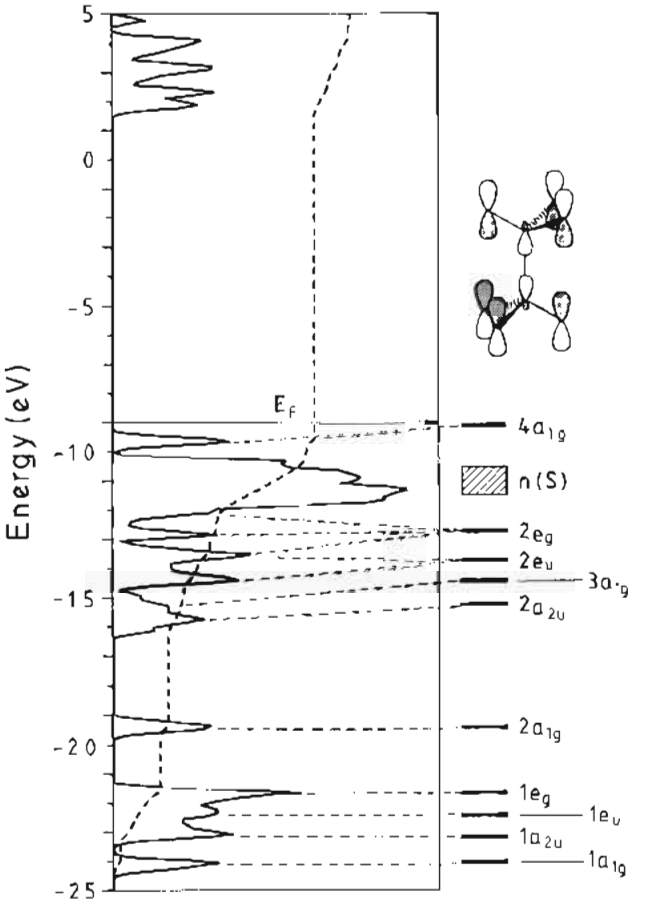

Figure 2. Density of states of the low-temperature (rhombohedral) phase of $CdPS_3$, calculated with the EHTB method. At the right are shown the energy levels of the molecular orbitals of an isolated $P_2S_6^{4-}$ ion. The dotted lines indicate the major contributions of such fragment molecular orbitals to the DOS of $CdPS_3$.

CdL_6 group with only the valence 5s and 5p atomic orbitals of the Cd atom and σ-type, lone-pair orbitals at each ligand. In main group metal ions such as Cd^{2+}, the valence d orbitals are too low in energy[20] to have any significant contribution to the SOJT term.[21–24] The molecular orbitals (MO's) of the CdL_6 group can be schematically represented as in **1** (actually obtained from EH calculations on a model $[CdS_6]^{10-}$ ion).

The results obtained for the molecular models will be checked by electronic band calculations for the low-temperature phase of $CdPS_3$. Therefore, we briefly describe here the electronic structure of $CdPS_3$. Its electronic dispersion diagrams, calculated with the LMTO and EH methods, are similar in all qualitative aspects. The semiconducting character of this compound is correctly predicted from both calculations, although the energy gap is underestimated (1.3 eV) by LMTO calculations and largely overestimated by the EH study (12 eV) as compared to the experimental absorption edge at 3.5 eV.[25] A good agreement between the EHTB calculated gap and the experimental value can be obtained by adjusting the Cd atomic parameters,[19] but we have chosen to keep the atomic parameters unchanged. The Cd 4d bands calculated at the LMTO level practically do not mix with other bands, thus confirming our previous assumption.

(16) Lee, S.; Colombet, P.; Ouvrard, G.; Brec, R. *Inorg. Chem.* **1988**, *27*, 1291–1294.
(17) Kurita, N.; Nakao, K. *J. Phys. Soc. Jpn.* **1989**, *58*, 232, 610.
(18) Whangbo, M.-H.; Brec, R.; Ouvrard, G.; Rouxel, J. *Inorg. Chem.* **1985**, *24*, 2459.
(19) Mercier, H.; Mathey, Y.; Canadell, E. *Inorg. Chem.* **1987**, *26*, 963.
(20) Alemany, P.; Alvarez, S. *Solid State Commun.* **1992**, *83*, 447–450.
(21) Bartell, L. S. *J. Chem. Educ.* **1968**, *45*, 754.
(22) Burdett, J. K. *Molecular Shapes*; J. Wiley: New York, 1980.
(23) Jahn, H. A.; Teller, E. *Proc. R. Soc. London* **1937**, *A161*, 220.
(24) Pearson, R. G. *J. Am. Chem. Soc.* **1969**, *91*, 4947.
(25) Brec, R.; Ouvrard, G.; Louisy, A.; Rouxel, J.; LeMehaute, A. *Inorg. Chem.* **1982**, *18*, 185.

Since the interaction between Cd^{2+} and the $P_2S_6^{4-}$ groups has an important ionic character, one can assign the occupied bands to the bonding and nonbonding molecular orbitals of the anions and the empty bands to the Cd^{2+} atomic orbitals and to the antibonding molecular orbitals of the anions. Such correlation is indicated in Figure 2 by the dashed lines connecting the low-lying bands of $CdPS_3$ and the energies of the corresponding MO's of $P_2S_6^{4-}$. In particular, the seven lowest bands are built up mainly from the seven bonding molecular orbitals of $P_2S_6^{4-}$: $1a_{1g}$, $1a_{2u}$, $1e_u$, $1e_g$, and $2a_{1g}$. The rest of the occupied bands are built up from approximately nonbonding orbitals, localized mostly at the sulfur atoms, if somewhat stabilized through mixing with the empty orbitals of the Cd^{2+} ions. Formally, these orbitals correspond to the 18 lone pairs ascribed to the sulfur atoms in a Lewis formula for $P_2S_6^{4-}$. A correlation can be established between the MO's of CdL_6 (**1**) and specific bands in Figure 2: the t_{1u} orbitals of ML_6 are within the n(S) block (Figure 2), whereas the a_{1g} MO mixes with the σ(P−P) orbital and appears at higher energy in $CdPS_3$ as the $4a_{1g}$ band. Finally, the a_{1g} and t_{1u} antibonding MO's of CdL_6 give place to the high-energy bands (above 0 eV).

Jahn−Teller Effect on Octahedrally Coordinated Cd^{2+}

Taking into account that the second-order Jahn−Teller effect is weighted by the difference in energy between the emtpy and occupied orbitals being mixed through a distortion, a mode of T_{1u} or T_{2u} symmetry is expected. The three degenerate T_{1u} modes correspond to the displacement of the Cd atom along any of the 3-fold axes of the octahedron. One of the T_{1u} modes is schematically represented in **2a**. We will not consider the

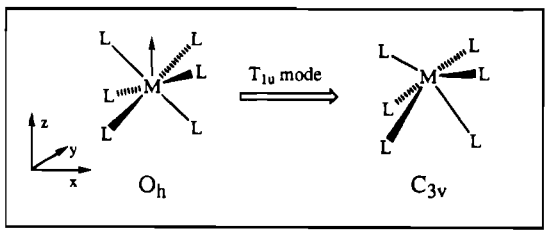

2a

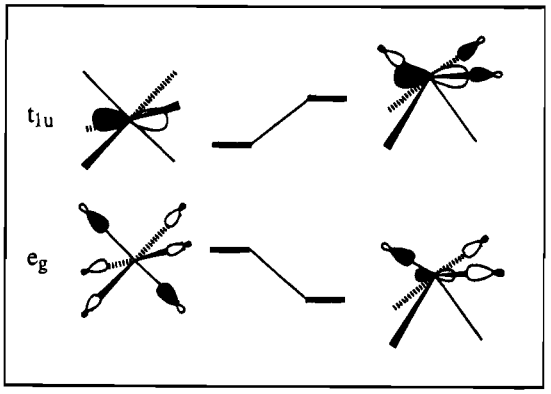

2b

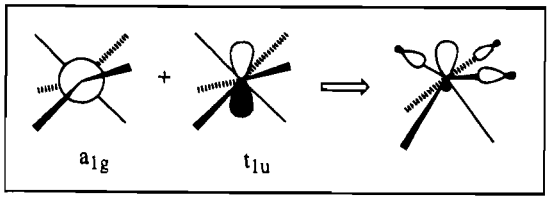

2c

T_{2u} mode in what follows because its effect is seen to be much less important in $CdPS_3$, both from the experimental data[7] and from our band calculations below. The total one-electron energy of $[CdS_6]^{10-}$ (without Cd 4d orbitals in the basis set; see below) was calculated (EH) as a function of the displacement of the Cd atom along the z axis and found to decrease upon distortion, giving a minimum for an off-center shift of ~1.8 Å, with the Cd atom slightly above one of the triangular faces, outside the octahedron. Although these results are biased by the neglect of core−core repulsions in EH calculations, they are clearly indicative of a tendency of the Cd atom to shift away from the octahedral site and suggest that for smaller ions, such as Cu(I), larger shifts can occur.

Band calculations at the EH level on the rhombohedral (low-temperature) phase of $CdPS_3$ also predict the structure to be stabilized when the Cd ions are displaced from the center of the octahedron along the c direction. Since the Cd shift is overestimated in this calculations (2.0 Å) for reasons given above, we have also carried out LMTO-ASA calculations in order to obtain a better quantitative estimate. The calculated shift of 0.2 Å (resulting in a net stabilization of 0.2 eV) nicely agrees with the refined structure of the low-temperature phase, in which the Cd atoms are shifted 0.1 Å in the same direction.[7] Furthermore, the fact that practically the same results are obtained when the Cd 4d orbitals are omitted confirms the above qualitative analysis for the molecular case, in the sense that the second-order Jahn−Teller distortion of the CdS_6 octahedra is not associated with the Cd 4d orbitals. Finally, the fact that molecular orbital and band structure calculations give the same result confirms that the observed Jahn−Teller distortion is essentially a local effect.

The existence of such a SOJT effect is in agreement with the elongated pdf ellipsoid found for $CdPS_3$ in its high-temperature phase and the two off-center sites found for Cd in the low-temperature phase.[6] The core−core repulsions neglected by the EH calculations effectively forbid the Cd atoms to shift all the way to the center of the S_3 triangles. This SOJT effect is also consistent with the existence of many structures of the MPS_3 family in which a d^{10} ion appears to be shifted, to be disordered, or to possess large thermal parameters along the c direction. Single-crystal studies of $AgMP_2S_6$ (M = V, Cr, In)[26,27] show that the silver cations present large atomic displacement parameters that can be modeled by several off-center positions. In $CuInP_2S_6$, the Cu(I) ions are distributed in two inequivalent off-center sites with occupation ratios of 0.875 and 0.1 per octahedron.[28] In another Cu(I) compound, $CuCrP_2S_6$, the electronic distribution of copper can be modeled by two positions close to the centers of the octahedra and two more near the opposite triangular faces,[29,30] whereas an additional pair of tetrahedral positions in the van der Waals gap was necessary for the refinement of the structure of $CuVP_2S_6$.[31,32]

It is worth trying to unravel the orbital nature of the second-order Jahn−Teller effect evidenced by the above calculations, keeping in mind that it must be associated with the Cd s and p orbitals, since d orbitals have not been considered in the present EH calculations. The T_{1u} mode lowers the symmetry of the

(26) Colombet, P.; Leblanc, A.; Ouvrard, G.; Brec, R. *Nouv. J. Chim.* **1983**, *7*, 333.
(27) Colombet, P. Personal communication, 1994.
(28) Maisonneuve, V.; Evain, M.; Payen, C.; Cajipe, V. B.; Molinié, P. *J. Alloys Compd.*, in press.
(29) Maisonneuve, V.; Cajipe, V. B.; Payen, C. *Chem. Mater.* **1993**, *5*, 758.
(30) Colombet, P.; Leblanc, A.; Danot, M.; Rouxel, J. *J. Solid State Chem.* **1982**, *41*, 174.
(31) Durand, E.; Ouvrard, G.; Evain, M.; Brec, R. *Inorg. Chem.* **1990**, *29*, 4916.
(32) Burr, G. L.; Durand, E.; Evain, M.; Brec, R. *J. Solid State Chem.* **1993**, *103*, 514.

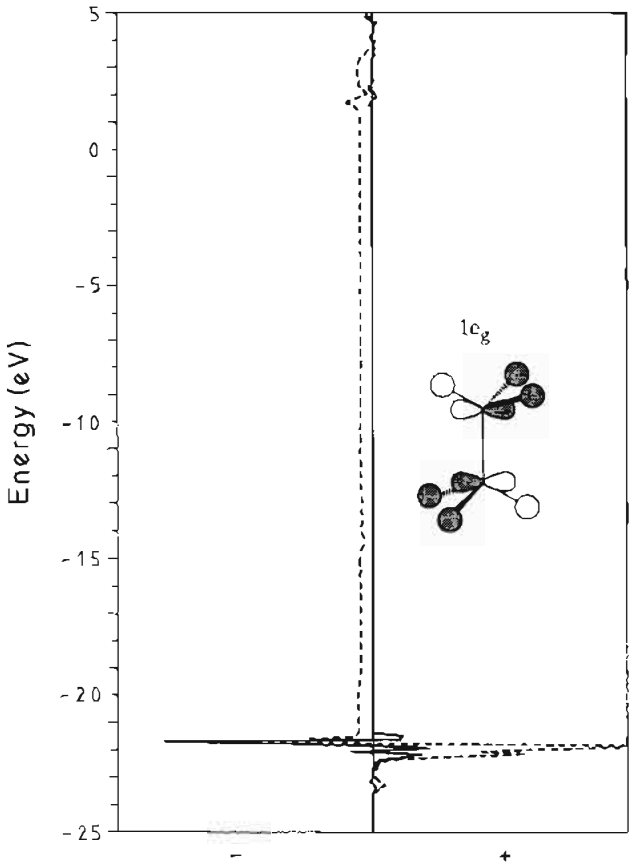

Figure 3. Crystal orbital displacement (COD, solid line) curve of the $1e_g$ fragment orbital of $P_2S_6^{4-}$ groups in $CdPS_3$ for the shift of Cd atoms 0.1 Å away from the octahedral position in the c direction (EHTB calculation). Positive sign indicates buildup; negative sign, decrease of $1e_g$ contribution on shifting the Cd atoms. The integral of the COD function (ICOD) is represented by the dashed line.

CdL_6 group from O_h to C_{3i}, thus allowing mixing of the nonbonding ligand orbitals e_g with the Cd t_{1u} (p_x and p_y) atomic orbitals (**2b**). In addition, the t_{1u} ($5p_z$) atomic orbital of Cd can be hybridized by mixing with the 5s (a_{1g}) orbital (**2c**), thus improving the interaction with the appropriate symmetry-adapted combination of the donor orbitals of the ligands. Put in simple terms, the second-order Jahn–Teller effect in an ML_6 complex of a main group element tends to optimize bonding between the metal p orbitals and the ligands by adopting a trigonal-pyramidal geometry. Although the underlying principles are the same as for d^{10}-ML_4[33] or d^0-ML_6 compounds,[34] the geometrical consequences are clearly different because of the different molecular orbitals involved in each case.

The same orbital explanation for the SOJT distortion is obtained from calculations on the full lattice by using crystal orbital displacement (COD) curves for the appropriate atomic or fragment orbitals.[35] The mixing of Cd p_x,p_y and the $P_2S_6^{4-}$ $1e_g$ orbitals can be seen in the COD plot for the latter (Figure 3). The features at −22 eV are indicative of a stabilization of band levels formed by $1e_g$.[35] Additionally, the negative value of ICOD at the Fermi level reveals the mixing of $1e_g$ levels into the Cd empty bands.

Comparison of the Two Phases

In this section we try to discern whether the different stacking of the layers associated with the phase transition is related to the second-order Jahn–Teller effect or not. It is therefore interesting to discover whether the different stacking pattern introduces any significant change in the electronic structure and to explore the possibility of identifying specific orbital interactions between the layers by performing COD and COOP analyses of EH tight-binding calculations.

In the monoclinic structure, the analysis of the interaction between layers was carried out by means of the corresponding COD[35] and COOP[36–38] curves. These confirm that the HOB is stabilized relative to the rhombohedral structure, through mixing with the band composed of the LUMO's of $P_2S_6^{4-}$ (see the COD curve, Figure 4, left). This interaction can be easily understood by looking at the topology of both HOMO and LUMO, schematically shown in **3**. Opposing the bonding

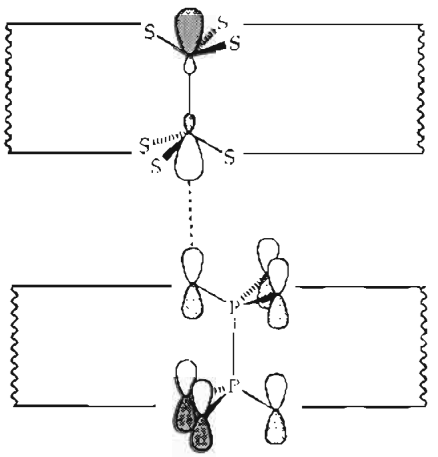

3

interaction between neighboring layers is the repulsion between the $1a_{2u}$ and $2a_{1g}$ electron pairs, identified by the bonding and antibonding P···S contributions at −23 and −19 eV, respectively, in the COOP curve (Figure 4, right).

The rhombohedral structure is calculated to be 0.30 eV more stable per unit cell than the monoclinic one. Clearly, the higher stability of the rhombohedral phase is not primarily due to the shift of the Cd atoms from the center of the S_6 octahedra, since their displacement by 0.1 Å represents a variation in the one-electron energy of only 0.05 eV in the EHTB calculations. This result agrees with the rhombohedral structure being the one observed at low temperature. However, it has not been possible to single out an interlayer orbital interaction responsible for the higher stability of the low-temperature phase.

Our interpretation of these results is that the rhombohedral stacking allows a closest packing of the layers (s = 3.125 Å, Figure 1) without making short S···S contacts (shortest contact 3.745 Å) responsible for lone-pair repulsions and without P···S bonding due to the long P–S interatomic distances (4.261 and 4.326 Å). The monoclinic stacking, with a larger separation between layers (s = 3.190 Å, Figure 1), presents slightly shorter S···S contacts (3.718 Å), compensated in part by the HOMO/LUMO interaction. It appears that the interlayer bonding and the relative stability of the two phases result from a delicate balance among the sulfur lone-pair repulsions, the HOMO/LUMO orbital interaction, and van der Waals interactions not accounted for by the present calculations.

(33) Burdett, J. K.; Eisenstein, O. *Inorg. Chem.* **1992**, *31*, 1758.
(34) Kang, S. K.; Tang, H.; Albright, T. A. *J. Am. Chem. Soc.* **1993**, *115*, 1971.
(35) Ruiz, E.; Alvarez, S.; Hoffmann, R.; Bernstein, J. *J. Am. Chem. Soc.* **1994**, *116*, 8207.
(36) Hughbanks, T.; Hoffmann, R. *J. Am. Chem. Soc.* **1983**, *105*, 3528.
(37) Hoffmann, R. *Solids and Surfaces: A Chemist's View of Bonding in Extended Structures*; VCH Publishers: New York, 1988.
(38) Wijeyesekera, S. D.; Hoffmann, R. *Organometallics* **1984**, *3*, 949.

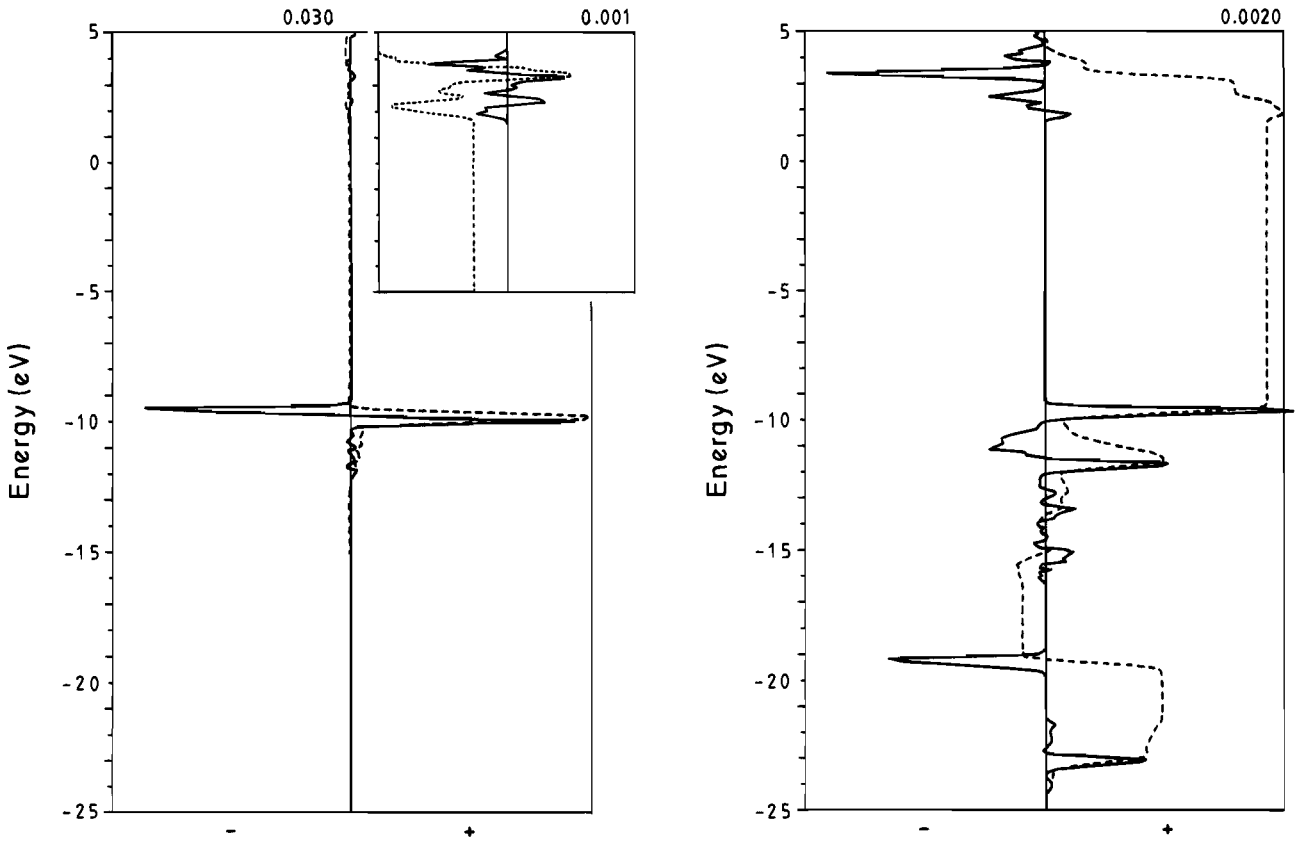

Figure 4. Left: COD (solid line) and ICOD (dashed line) curves of the $4a_{1g}$ orbital of $P_2S_6^{4-}$ for the rhombohedral to monoclinic phase transition of $CdPS_3$. The inset is a blow-up of the high-energy region of the same COD and ICOD curves. The numbers at the top of the diagrams correspond to the COD values for the full scale (in number of levels). Right: Crystal orbital overlap population (COOP) curve for the interlayer P···S interaction in the monoclinic (high-temperature) phase of $CdPS_3$.

Computational Aspects

Linear muffin-tin orbital calculations have been carried out in an atomic sphere approximation (LMTO-ASA) with a basis of almost orthogonal muffin-tin orbitals.[39] Since this method is best suited for close-packed structures,[40] we have filled the van der Waals gap with "ghost" atoms. The radii of the Wigner–Seitz atomic spheres were taken as $R(P) = 1.4$ Å, $R(Cd) = R(S) = R(ghost) = 1.84$ Å. Larger values for $R(P)$ could not be used to avoid having the phosphorus spheres intersect with the core levels of other atomic spheres. The radii chosen for the other atoms provide complete filling of the crystal volume, to fulfill a usual condition of the LMTO-ASA method. The use of the LMTO-ASA one-electron energies for the study of the off-center shift of Cd is meaningful according to Andersen's *local force* theorem,[41] which states that the changes in total energy for small distortions of the crystal are equal to the changes in one-electron energy within the local density functional theory.

Tight-binding band calculations within the extended Hückel framework[42,43] were carried out using the weighted Wolfsberg–Helmholz formula for the nondiagonal elements of the Hamiltonian matrix[44] and the atomic parameters from the literature.[20,45] The calculations of properties (total one-electron energy, Mulliken population analysis, density of states, and COD curves) were carried out using grids of 27 **k**-points in the irreducible wedge of the Brillouin zone.

Acknowledgment. Financial support to this work was provided by the DGICYT through Grant PB92-0655. V.Z. thanks the Ministerio de Educación y Ciencia (Spain) for a sabbatical grant. The authors are grateful to F. Vilardell for expert drawings and to E. Ruiz for many helpful discussions.

IC940868O

(39) Andersen, O. K.; Jepsen, O.; Glotzel, D. *Highlights of Condensed Matter Theory*; Societá Italiana di Fisica: Bologna, Italy, 1985.
(40) Andersen, O. K. *Phys. Rev. B* **1975**, *42*, 3060.
(41) Mackintosh, R.; Andersen, O. K. In *Electrons at the Fermi Surface*; Springford: London, 1980; p 57.
(42) Whangbo, M.-H.; Hoffmann, R. *J. Am. Chem. Soc.* **1978**, *100*, 6093.
(43) Hoffmann, R. *J. Chem. Phys.* **1963**, *39*, 1397.
(44) Wolfsberg, M.; Helmholtz, L. *J. Chem. Phys.* **1952**, *20*, 837.
(45) Boucher, F.; Evain, M.; Brec, R.; Mathey, Y. *Eur. J. Solid State Inorg. Chem.* **1991**, *28*, 383.